9th Asia-Pacific Conference on Wind Engineering
Auckland, New Zealand
3-7 December 2017

Experimental Study of a NACA0015 Circulation Control Aerofoil Using Synthetic Jets

P. Itsariyapinyo and R.N. Sharma

Mechanical Engineering
University of Auckland, Auckland 1142, New Zealand

Abstract

As opposed to a conventional aerofoil, the trailing edge of a circulation control aerofoil is rounded to make the Coanda surface. In this study, wind tunnel testing is carried out on a NACA0015 circulation control aerofoil to explore the possibility of replacing a continuous jet, which is commonly used on a circulation control aerofoil, with a synthetic jet. A free-stream velocity of 10 m/s, which is corresponding to the chord Reynolds number of 1.1×10^5, is used. The aerofoil is tested at the angles of attack of 0°-15°. In order to investigate the effects of excitation frequency and momentum coefficient on the lift coefficient, the synthetic jet is actuated at the excitation frequencies of 150-600 Hz and the momentum coefficient of 0.00056-0.0189. The results show that the lift coefficient could be increased by up to 23% when the synthetic jet is actuated at the reduced frequency of 0.14 which is close to the Strouhal number of 0.17 based on the diameter of the rounded trailing edge. Furthermore, the actuation is found to be most effective when the flow separation point is slightly upstream of the synthetic jet slots.

Introduction

A circulation control aerofoil was proposed in the early 20th century. The initial concept emerged from a simple experiment in which a sign of lift enhancement was detected when a continuous jet was blown on the surface of an aerofoil. To date, a circulation control aerofoil has seen much progress including many successful experiments which has led to its instalments on aircraft [4]. Nevertheless, its reliance on complicated mechanical components, such as an auxiliary compressor, has rendered the system less practical and such problem shall persist for as long as a continuous jet is used.

Conventionally, a circulation control aerofoil consists of an air plenum and an orifice. Compressed air is usually either supplied from a compressor or a propulsive system to produce an air jet. Upon ejecting an air jet onto the Coanda surface, this air jet is then entrained on the surface and eventually detached from the surface when its momentum is depleted. Through this process, a separation point or a rear stagnation point on a circulation control aerofoil could be deliberately altered according to the momentum of an air jet. Consequently, the lift coefficient could be increased due to an improved circulation.

In addition to a rather complicated system of a conventional circulation control aerofoil, a continuous jet lacks the oscillatory behaviour which is crucial for exploiting flow instabilities, such as vortex shedding. Since flow instabilities are characterised by collections of fluctuating pressure waves, the periodic injection of momentum at the frequency close to the dominant frequency of these pressure waves could provide significant improvement on a circulation on an aerofoil.

Unlike a continuous jet, a synthetic jet can be conveniently produced by a simple actuator which consists of a cavity, an orifice, and an oscillating membrane (small loudspeaker in this study). In most investigations, oscillating membranes are usually driven by a signal generator and a power amplifier. Due to these advantages, the current study introduces a synthetic jet to the circulation control aerofoil so that its performance could be investigated.

Experimental Setup

The dimensions of the circulation control aerofoil are designed according to Englar's hypothesis [1]. Thus, the aerofoil chord length of 170 mm, the Coanda radius of 4 mm, and the jet slot width of 0.2 mm are chosen. A total number of 73 pressure taps are built at the mid-span of the aerofoil. A single tap is placed at the leading edge of the aerofoil. 31 and 30 taps are placed on the suction and pressure sides, respectively. 11 taps are placed at the round trailing edge or the Coanda surface. In this region, the taps are spaced by 15° apart. The aspect ratio of the aerofoil is chosen to be 6.6, which yields the wing span of 1122 mm, to achieve two-dimensional flow. A free-stream velocity of 10 m/s, which is corresponding to the chord Reynolds number of 1.1×10^5, is used. The aerofoil is tested at the angles of attack of 0°-15°. In order to investigate the effects of excitation frequency and momentum coefficient (C_μ), the synthetic jet is actuated at the excitation frequencies of 150-600 Hz and the momentum coefficient of 0.00056-0.0189.

The governing parameters of a synthetic jet are the excitation frequency and the momentum coefficient. In most investigations which concern active flow control, the excitation frequency of most flow control devices is usually normalised or reduced by a characteristic length. For instance, the control of flow separation using a synthetic jet usually uses the distance from a jet slot to the trailing edge of an aerofoil as its characteristic length. However, because the jet slots of the circulation control aerofoil are located too close to the trailing edge, the diameter of the Coanda surface is used as a characteristic length instead. The reduced frequency (F^+) used in this paper is as follows

$$F^+ = fd/U_\infty \tag{1}$$

where f is the excitation frequency, d is the diameter of the Coanda surface, and U_∞ is a free-stream velocity.

Likewise, the frequencies of the flow instabilities are normalised in the same manner to obtain their corresponding Strouhal numbers (Sr) which are estimated from

$$Sr = fd/U_\infty \tag{2}$$

where f, in this formula, is the flow instability's frequency.

In order to establish a universal measure for the jet momentum which could be used for benchmarking, the momentum coefficient could be estimated from

$$C_\mu = \bar{I}_j / 0.5\rho_\infty U_\infty^2 c \tag{3}$$

$$\bar{I}_j = \frac{1}{T/2}\rho_j b \int_0^{T/2} u_j^2(t)dt \qquad (4)$$

where $\bar{I}_j$ is the time-averaged jet momentum per unit length during the expulsion stroke, ρ_∞ is a free-stream density, c is the aerofoil chord length, T is the period of the synthetic jet actuation, ρ_j is the jet density, b is the width of the jet slot, and u_j is the jet velocity.

The objective of the experiment is to study the effects of excitation frequency and momentum coefficient on the lift coefficient. Pressure distributions of the aerofoil are acquired from the pressure taps which are sampled by the pressure system at the University of Auckland. The lift coefficient is estimated from the pressure distribution. In addition to an investigation on the effects of synthetic jet actuation, the flow instabilities' frequencies are determined to provide some insights into how these frequencies may influence the operation of circulation control. In order to estimate the shear-layer instability frequency, the pressure spectra are obtained from the surface pressures which are sampled from each pressure tap at 4096 Hz for 10s. On the other hand, the vortex shedding frequency is estimated from the velocity spectra which are obtained at x/c = 3.00. TFI cobra probe (series 100) is used to sample the wake velocity at 1024 Hz for 33s. A laboratory computer is equipped with a 14 bit 48 kHz National Instruments USB-6009 A/D board to enable high frequency response.

Results

Effective flow control usually requires one's knowledge on the dominant frequency of a wetted object. Since such frequency could either be the frequency which is proportional to the characteristic length of an object or the frequency which arises from flow instabilities, this dominant frequency could possibly be determined by trial-and-error method and spectral analysis. In trial-and-error method, the synthetic jet actuations of fixed momentum coefficient are performed at a frequency range of 150-600 Hz. The excitation frequency which could yield the highest lift coefficient is considered to be the dominant frequency. On the other hand, the spectral analyses of the pressure and velocity spectra of the aerofoil are carried out to search for any frequency which exhibits high power amplitude. Furthermore, it is of interest that the laminar separation bubble on the low Reynolds number aerofoil is studied as its existence may affect the effectiveness of the synthetic jet actuation.

Characteristics of the Laminar Separation Bubbles

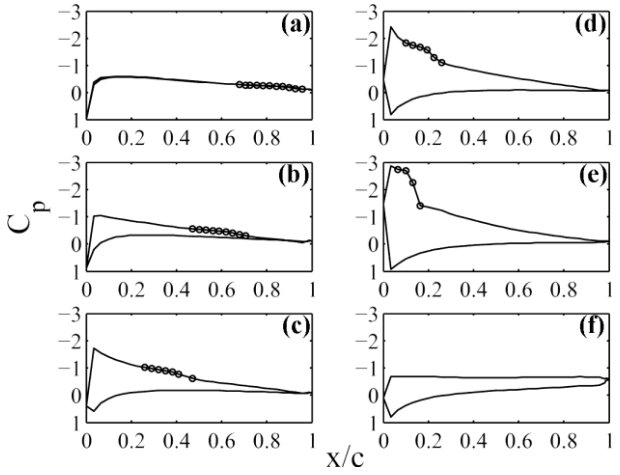

Figure 1. Pressure distributions of the non-actuated circulation control aerofoil at α = (a) 0°, (b) 3°, (c) 6°, (d) 9°, (e) 12°, and (f) = 15°. Symbol o marks the streamwise extent of the laminar separation bubble

On a low Reynolds number aerofoil, a laminar separation bubble is usually expected and its existence could be confirmed by a "kink" on the pressure distribution [2]. As shown in figure 1, the length of the laminar separation bubble is marked by symbols o. At the point where the flow is separated, the laminar separation bubble begins to form. Followed by the flow separation point, a "plateau" of constant pressure is developed. At the point where the pressure begins to drop, the edge of a "plateau" represents the flow transition point. At the point where the pressure proceeds to follow the pressure recovery slope, this point is known as the flow reattachment point.

As shown in figure 1, the laminar separation bubble contracts in size and moves upstream as the angle of attack increases from α = 0° to 12°. As the aerofoil stalls at α = 15°, a short bubble "bursts" into a long bubble via the bubble bursting mechanism [2]. At this angle of attack, the length of the laminar separation bubble seems to have covered the entire suction side of the aerofoil.

Frequency of Shear-Layer Instability via Pressure Spectra

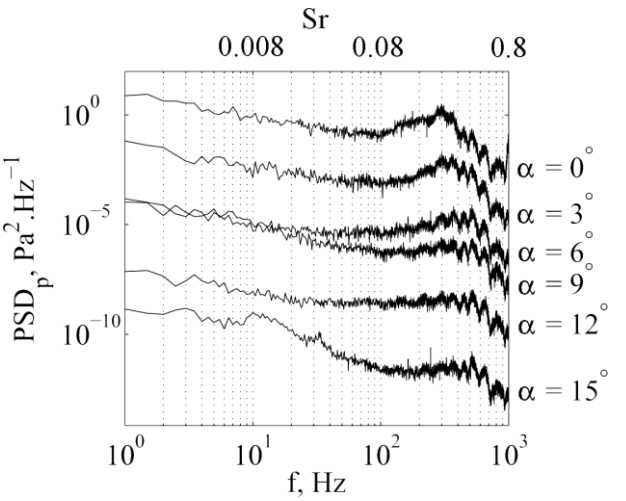

Figure 2. Surface pressure spectra obtained near the flow reattachment points. The amplitude of each consecutive trend is stepped down by an order of 0.01.

Within the flow separation region, the pressure spectra obtained from the flow reattachment points are observed to have formed the most well-defined spectral peaks. These well-defined spectral peaks imply that the pressure signals at the flow reattachment points might have developed series of sinusoidal-like waves. From this interpretation, it is likely that the periods of these sinusoidal waves may be associated with the shear-layer instability frequency or the dynamics of the roll-up vortices. In an attempt to estimate the shear-layer instability frequency, the surface pressures are sampled from several pressure taps to capture the activity of this flow instability which could possibly be reflected by the pressure signals. As shown in figure 2, the spectral peaks at α = 0°, 3°, 6°, 9°, 12°, and 15° are found at approximately 300, 367, 444, 460, 533, and 518 Hz, respectively. These frequencies are corresponding to the Strouhal numbers of 0.24, 0.29, 0.36, 0.37, 0.43, and 0.41, respectively.

Interestingly, 2 spectral peaks at 33 Hz and 511 Hz are found on the pressure spectra at α = 15°. While the high-frequency spectral peak may be associated with the shear-layer instability frequency, the low-frequency spectral peak is likely to be associated with the vortex shedding frequency. The appearance of the low-frequency spectral peak is possibly due to the effects of bluff body which will be further discussed in the next section. According to the results, it is fair to say that the shear-layer instability frequency increases as the angle of attack increases. Hence, such information implies that vortices roll up more frequently at high angles of attack.

Frequency of Vortex Shedding via Velocity Spectra

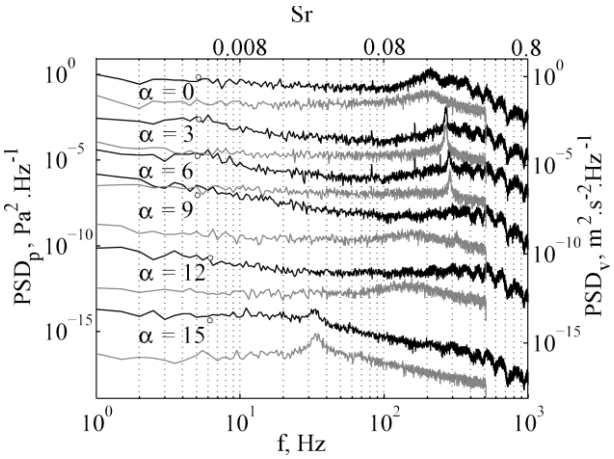

Figure 3. Surface pressure spectra (black) obtained at x/c = 0.99 and vertical wake velocity spectra (grey) obtained at x/c = 3.00. The amplitude of each consecutive trend is stepped down by an order of 0.01.

Followed by the roll-up of vortices, there is a good chance that the subsequent roll-up vortex could catch up and merge with the preceding roll-up vortex. In such occasion, the spectral peak at a lower frequency is usually formed downstream at the point where vortices merge [3]. Since the spectral peak at a lower frequency continues to exist until x/c = 3.00, it is only fair to consider this frequency as the vortex shedding frequency.

At low angles of attack where the flow separation points occur very close to the trailing edge, the vortex shedding frequencies at these angles of attack are heavily dominated by the shear-layer instability mode. Thus, the vortex shedding frequencies at these angles of attack are considerably high. On the other hand, the vortex shedding frequency tends to decrease as the angle of attack increases. By increasing the angle of attack, the advection length which the vortices have to travel becomes longer as the laminar separation bubble moves further upstream. As a result, such has increased the likelihood that the subsequent vortex will catch up and merge with the preceding vortex. Hence, the effects of bluff body have become more dominant at high angles of attack.

As shown in figure 3, the vortex shedding frequencies at α = 0°, 3°, 6°, 9°, 12°, and 15° are approximately 210, 271, 284, 155, 138, and 33 Hz, respectively. These frequencies are corresponding to the Strouhal numbers of 0.17, 0.22, 0.23, 0.12, 0.11, and 0.03, respectively. From α = 6° to 9°, a drastic drop in the frequency is quite evident and this is likely due to vortex merging which seems to have become more influential as the aerofoil starts to behave like a bluff body. At the stall angle of attack (α = 15°), the effects of bluff body have become very evident as the vortex shedding frequency has dropped to 33 Hz. Overall, the spectral peaks presented by the wake velocity spectra agree well with those of the pressure spectra.

Effects of Excitation Frequency on the Lift Coefficient

As shown in figure 4, the excitation frequency at 175 Hz, which corresponds to $F^+ = 0.14$, is found to have achieved the highest lift coefficient for most angles of attack. The degree of lift enhancement is observed to have declined as the excitation frequency increases beyond the dominant frequency of 175 Hz. Nevertheless, it is noteworthy that the synthetic jet actuation has partially regained its effectiveness at the subharmonic frequency of approximately 350 Hz. Though such evidence is not provided in this paper, an increment in the lift coefficient is characterised by an increase in the pressure gradient between the suction and pressure sides of the aerofoil.

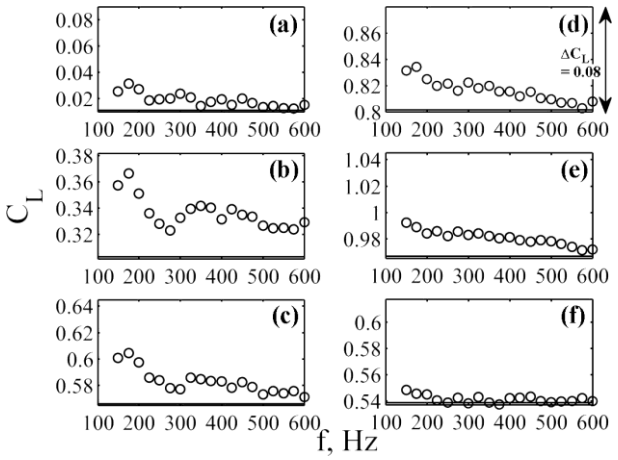

Figure 4. Variations of lift coefficients at α = (a) 0°, (b) 3°, (c) 6°, (d) 9°, (e) 12°, and (f) = 15° due to the excitation frequency at the fixed momentum coefficient of 0.00392. The solid lines located below scatters mark the non-actuated lift coefficients.

The results, so far, have made it clear that the choice of the excitation frequency is vital to flow control. Knowing that the dominant frequency could yield the highest lift coefficient, the remainder of this section shall be dedicated to an attempt to provide a simple approximation of the dominant frequency. The hypothesis of the current study states that the dominant frequency, which is the frequency that could yield the highest lift coefficient, may either be dependent on the characteristic length of that object or the flow instabilities' frequencies which are considerably sensitive to a change in the angle of attack. In this case where the dominant frequency is fixed at 175 Hz for α = 0°-9°, it is highly possible that the dominant frequency of this particular aerofoil is dependent on some characteristic length which seems to have remained almost constant at low angles of attack. Since the trailing edge of this aerofoil is similar to that of a circular cylinder, we shall now scope our interest to that of a circular cylinder. According to the classical work conducted by Roshko [5], the wake width of a circular cylinder is found to be proportional to the vortex shedding frequency. In order to ensure that the diameter of the circular cylinder at the trailing edge is least affected by the geometrical parameters and the angle of attack of the aerofoil, the vortex shedding frequency of 210 Hz (Sr = 0.17) at α = 0° is chosen to represent the vortex shedding frequency which could possibly be produced by a conventional circular cylinder of the same Reynolds number. Provided that such Strouhal number is constant at any angle of attack and that the vortex shedding frequency and the wake width change accordingly, it would seem that the wake width remains relatively consistent until the aerofoil begins to behave like a bluff body at α > 9°. It is probably due to this reason that exciting the synthetic jets at 175 Hz on the aerofoil at α > 9° does not yield decent lift enhancement. Nevertheless, it is noteworthy that the universal Strouhal number of 0.20 and the diameter of a circular cylinder may be cautiously used to predict the vortex shedding and dominant frequencies as their values are observed to be within a similar range (Sr = 0.14-0.20).

Effects of Momentum Coefficient on the Lift Coefficient

Figure 5 shows the variations of lift coefficients due to the synthetic jet actuations of different momentum coefficients. The results reveal that the excitation at the dominant frequency of 175 Hz yields the steepest $\Delta C_L/\Delta C_\mu$ slope and this slope is observed to have declined as the excitation frequency increases. Thus, it could be concluded that the momentum coefficient serves its role by amplifying the effects which are predetermined by the excitation frequency. Provided that the synthetic jet is actuated at the dominant frequency, the minimum amount of momentum coefficient is required to achieve high degree of lift enhancement.

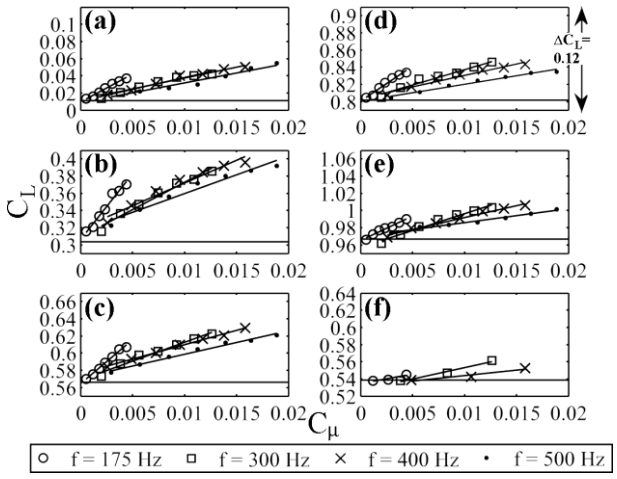

Figure 5. Variations of lift coefficients at α = (a) 0°, (b) 3°, (c) 6°, (d) 9°, (e) 12°, and (f) = 15° due to the excitation frequencies and momentum coefficients. The solid lines located below scatters mark the non-actuated lift coefficients.

Effects of Excitation Location on the Synthetic Jet Actuation

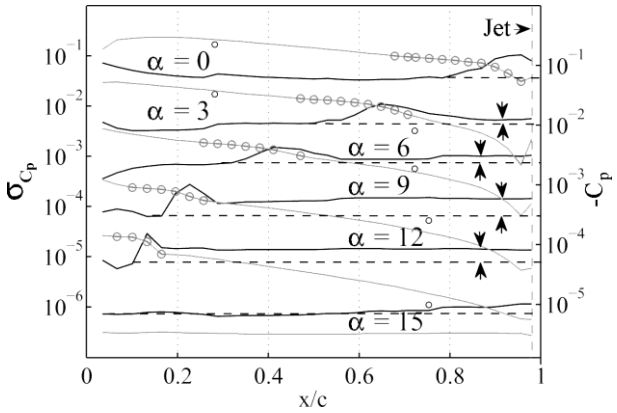

Figure 6. Locations of flow separation as indicated by the standard deviations of time-history pressure coefficients (black) and the time-averaged pressure coefficients (grey) on the suction side of the aerofoil. Symbol o marks the streamwise extent of the laminar separation bubble on the aerofoil. The amplitude of each consecutive standard deviation trend is stepped down by order of 0.1. The amplitude of each consecutive pressure coefficient trend is stepped down by 0.5, 0.05, ….

Figure 6 shows the standard deviations of the fluctuating pressure coefficients and the time-averaged pressure coefficients on the suction side of the aerofoil. It is noticeable from this figure that a "kink" in the pressure distribution represents the laminar separation bubble and that a sudden increase in the standard deviation is developed at around the points of transition and flow reattachment. Prior to the flow separation, the flow is presumably laminar. Thus, the standard deviations in this region are considerably low. At the flow separation region, sudden increase and decrease in the standard deviation are found at around the points of transition and flow reattachment, respectively. Interestingly, it is noted that the peak of the standard deviation formed at these regions increases as the angle of attack increases. After the flow reattachment, the flow is considered to be turbulent and such state could be indicated by a relatively high standard deviation. Although the standard deviation drastically drops at the flow reattachment point, the standard deviations in the turbulent region would still always be higher than those in the laminar region. At low angles of attack, the differences between the standard deviations in the laminar and turbulent regions are relatively small. Upon increasing the angle of attack, such differences gradually increase until they become very obvious at α = 9° and 12°. As the laminar separation bubble bursts and the pressure distribution on the suction side is flattened at α = 15°, there is no peak of standard deviation developed on the stall aerofoil. Instead, the standard deviation steadily increases from the leading edge to the trailing edge of the aerofoil. As a result, the pressure fluctuations become extremely turbulent at the trailing edge.

According to the aforementioned report, it is, so far, fair to say that the effectiveness of the synthetic jet actuation is somewhat sensitive to the fluctuations of surface pressure. The reason why the synthetic jet actuation at α = 3° yields the highest degree of lift enhancement is possibly due to the fact that the jet slots are located in the region of low turbulence. Although it was initially anticipated that the synthetic jet actuation at α = 0° would yield the highest degree of lift enhancement, this does not seem to be the case as the flow separation region is developed at the jet location. Thus, the jet slots on the aerofoil at α = 0° are fully exposed to high turbulence. At α = 3°, a region of high turbulence moves upstream and the jet slots are located at the area where the turbulence has already calmed down. Even though the turbulence at high angles of attack has also gone down by the time it reaches the jet slots, it should be pointed out that the turbulence at these high angles of attack is still comparatively much higher than that at α = 3°. Therefore, the effectiveness of the synthetic jet actuation may continue to fall as the turbulence at the jet location continues to rise.

Conclusions

The highest lift coefficients are observed to have been achieved at α = 0°-9° when the synthetic jets are actuated at 175 Hz ($F^+ = 0.14$). According to the setup of this study, the excitation frequency at 175 Hz is corresponding to $F^+ = 0.14$ which is considerably close to Sr = 0.17 based on the diameter of the circular cylinder. Since the excitation frequency at 175 Hz continues to yield the highest lift coefficient for the aerofoil at α = 0°-9°, its consistency implies that the dominant or the most effective excitation frequency is more dependent on the diameter of the rounded trailing edge than the flow instabilities' frequencies which change according to the angle of attack. Upon actuating the synthetic jets at the frequency which is higher than the dominant frequency, the degree of lift enhancement is worsened as the excitation frequency increases. Depending on the effectiveness ($\Delta C_L/\Delta C_\mu$) of each excitation frequency, the lift coefficient increases almost linearly with the momentum coefficient. Furthermore, the most effective synthetic jet actuation could be achieved at α = 3° which is when the flow separation point is slightly upstream of the synthetic jet slots.

References

[1] Englar, R.J., *Two-Dimensional Subsonic Wind Tunnel Tests of Two 15-Percent Thick Circulation Control Airfoils*, David W. Taylor Naval Ship Research and Development Center Technical Note AL-211, Washington, DC, 1971.

[2] Gaster, M., Laminar separation bubbles, in *Sixth IUTAM Symposium on Laminar-Turbulent Transition*, editor R. Govindarajan, Springer, Netherlands, 2006, 1-13.

[3] Ho, C.M., Local and Global Dynamics of Free Shear Layers, in *Numerical and Physical Aspects of Aerodynamic Flows*, editor T. Cebeci, Springer-Verlag, New York, 1982, 521-533.

[4] Joslin, R.D., and Jones, G.S. (editors) *Applications of Circulation Control Technologies*, AIAA, Reston, VA, 2006.

[5] Roshko, A., *On the drag and shedding frequency of two-dimensional bluff bodies*, NACA-TN-3169, Washington, DC, 1954.